

Drp1 Loss-of-function Reduces Cardiomyocyte Oxygen Dependence Protecting the Heart From Ischemia-reperfusion Injury

Ramiro Zepeda, PhD,*† Jovan Kuzmicic, PhD,* Valentina Parra, PhD,*‡ Rodrigo Troncoso, PhD,* Christian Pennanen, PhD,* Jaime A. Riquelme, BSc,* Zully Pedrozo, PhD,*† Mario Chiong, PhD,* Gina Sánchez, PhD,*† and Sergio Lavandero, PhD*†‡

Abstract: Mitochondria are key organelles for ATP production in cardiomyocytes, which is regulated by processes of fission and fusion. We hypothesized that the mitochondria fusion protein dynamin-related protein 1 (Drp1) inhibition, attenuates ischemia-reperfusion (I/R) injury through modifications in mitochondrial metabolism. Rats were subjected to I/R through coronary artery ligation, and isolated cardiomyocytes were treated with an ischemia-mimicking solution. In vivo, cardiac function, myocardial infarction area, and mitochondrial morphology were determined, whereas in vitro, viability, mitochondrial membrane potential, intracellular ATP levels, and oxygen consumption rate (OCR) were assessed. In both models, an adenovirus expressing Drp1 dominant-negative K38A (Drp1K38A) was used to induce Drp1 loss-of-function. Our results showed that I/R stimulated mitochondrial fission. Myocardial infarction size and cell death induced by I/R were significantly reduced, whereas cardiac function after I/R was improved in Drp1K38A-treated rats compared with controls. Drp1K38A-transduced cardiomyocytes showed lower OCR with no decrease in intracellular ATP levels, and on I/R, a larger decrease in OCR with a smaller reduction in intracellular ATP level was observed. However, proton leak-associated oxygen consumption was comparatively higher in Drp1K38A-treated cardiomyocytes, suggesting a protective mitochondrial uncoupling effect against I/R. Collec-

tively, our results show that Drp1 inhibition triggers cardioprotection by reducing mitochondrial metabolism during I/R.

Key Words: mitochondria, metabolism, ischemia/reperfusion, Drp1, mitochondrial fission

(*J Cardiovasc Pharmacol*™ 2014;63:477–487)

INTRODUCTION

According to the World Health Organization, coronary heart disease and myocardial infarction are the leading cause of death worldwide, affecting 3.8 million men and 3.4 million women every year.¹ During myocardial infarction, cardiomyocyte metabolism is severely altered, because of the absence of oxygen, nutrients, and cell acidification.² In this context, mitochondria have emerged as one of the key organelles in cardiomyocytes because they are the main ATP source required for cardiac muscle contraction and survival.

Given the high density of mitochondria in cardiomyocytes and the absolute dependence on mitochondrial oxidative phosphorylation to generate ATP for cardiac contraction, it is not surprising that pathological alterations in this tissue are often associated with changes in mitochondrial metabolism or function.³ Changes in substrate utilization by the mitochondria, compromise of the electron transport chain, and decreased ATP synthesis capacity, result in a general deterioration of cardiac metabolic function.^{4,5} Furthermore, mutations that decrease mitochondrial oxidative phosphorylation or alter the activity of proteins involved in the transport of mitochondrial substrates (such as adenine nucleotide and fatty acid transporter proteins) can cause diverse cardiomyopathies.^{6–8}

Mitochondria are highly dynamic organelles that undergo continuous fusion and fission events.^{9,10} In mammals, fusion is mainly controlled by 3 different dynamin-related GTPase proteins, namely mitofusins 1 and 2 (Mfn1 and Mfn2) and the optic atrophy 1 protein (Opa1).^{9,11–13} Mfn1 and Mfn2 are localized in the outer mitochondrial membrane (OMM), interacting with each other to tether and fuse the OMM. Opa1 is localized in the intermembrane space, in tight association with the inner mitochondrial membrane¹⁴ and is essential to the formation and maintenance of mitochondrial cristae and the coordination of inner mitochondrial membrane fusion. In parallel, the proteins that regulate mitochondrial fission are the fission protein 1 (Fis1) and the dynamin-related

Received for publication July 22, 2013; accepted December 17, 2013.

From the *Advanced Center for Chronic Diseases and Centro Estudios Moleculares de la Célula, Facultad de Ciencias Químicas y Farmacéuticas and Facultad de Medicina, Universidad de Chile, Santiago, Chile; †Instituto de Ciencias Biomédicas, Facultad de Medicina, Universidad de Chile, Santiago, Chile; and ‡Department of Internal Medicine, Division of Cardiology, University of Texas Southwestern Medical Center, Dallas, TX.

Supplemental digital content is available for this article. Direct URL citations appear in the printed text and are provided in the HTML and PDF versions of this article on the journal's Web site (www.jcvp.org).

Supported by grants FONDAF 15130011 (S.L. and M.C.), Anillo ACT 1111 (S.L. and M.C.), FONDECYT 1120212 (S.L.), 1130407 (G.S. and S.L.), 3110114 (R.T.), 3110039 (Z.P.), 1110180 (M.C.), and 3130749 (C.P.) from CONICYT Chile.

J. Kuzmicic and J. A. Riquelme hold a PhD fellowship from CONICYT. V. Parra has postdoctoral fellowships from CONICYT. The remaining authors report no conflicts of interest.

Reprints: Sergio Lavandero, PhD, Advanced Center for Chronic Diseases & Centro Estudios Moleculares de la Célula, Facultad de Ciencias Químicas y Farmacéuticas & Facultad de Medicina, Universidad de Chile, Olivos 1007, Santiago 8380492, Chile (e-mail: slavander@uchile.cl).

Copyright © 2014 by Lippincott Williams & Wilkins

protein 1 (Drp1).¹⁰ Although Fis1 is uniformly located in the OMM, Drp1 is a cytosolic protein that is recruited in a punctuate fashion over the mitochondrial surface, marking the future sites of mitochondrial fission. The knockdown of either protein results in the elongation and increased interconnectivity of mitochondrial tubules.¹⁵ Moreover, alterations in both fusion and fission processes have been associated with several pathological heart conditions.^{16,17} For example, increased mitochondrial fission has been documented in models of ischemia/reperfusion (I/R), and pharmacological inhibition of the mitochondrial fission protein, Drp1, has been shown to reduce infarct size in mice subjected to coronary artery occlusion and reperfusion.¹⁷

Because the control of mitochondrial fission is the key for the correct function of mitochondria and the down-regulation of Drp1 triggers mitochondrial dysfunction, it is necessary to clarify whether the control of metabolism by mitochondrial dynamics is important in the I/R injury.

In this study, we show for the first time that inhibition of Drp1 reduces I/R injury through the decrease in the metabolic oxygen dependence of cardiomyocytes. Our results suggest that the manipulation of mitochondrial dynamics to reduce oxygen consumption during ischemia can be used as a strategy to preserve myocardial function.

METHODS

Ethics Statements

Rats were bred in the Animal Breeding Facility at the Faculty of Chemical and Pharmaceutical Sciences, University of Chile (Santiago, Chile). All animal procedures were performed following the "Guide for the Care and Use of Laboratory Animals" published by the US National Institutes of Health (NIH Publication, 8th Edition, 2011) and were approved by our Institutional Ethic Committee.

Cardiomyocyte Culture

Cardiomyocytes were prepared from hearts of neonatal (1- to 3-day old) Sprague-Dawley rats as described previously.¹⁸ Cardiomyocytes were plated at a final density of $1-8 \times 10^3/\text{mm}^2$ on gelatin-coated Petri dishes and were not cultured for more than 4 days. Cell cultures contained at least 95% cardiomyocytes.

Myocardial and Cardiomyocyte I/R

Male Sprague-Dawley rats (12–16 weeks, 200–250 g) were anesthetized with a combination of ketamine and xylazine injected intraperitoneally (0.01 mL/g body weight, 10 mg/mL ketamine, and 2 mg/mL xylazine), and body temperature was maintained at 37°C. Respiration was maintained at 60 strokes per minute, 220 μL per stroke using a rodent Minivent (Type 845; Harvard Apparatus, Kent, United Kingdom) with oxygen supplementation (1 L/min). A left anterior thoracotomy was performed, and a chest retractor was used to expose the heart. Ligation of the left anterior descending coronary artery was performed at ~ 2 mm below the tip of the left atria using a 8-0 prolene monofilament polypropylene suture.¹⁹ Reperfusion was done by the removal of the suture.

Infarcted and risk regions were measured with the triphenyl-tetrazolium staining technique.²⁰ After reperfusion, rats were euthanized by decapitation and hearts were collected. Myocardial infarction size was expressed as a percentage of the infarcted area normalized by the risk area. The risk area was expressed as percentage of the total left ventricular volume. In vitro simulated I/R was performed by incubating cardiomyocytes in an ischemia-mimicking solution containing (in millimolar) HEPES (5), 2-deoxy-D-glucose (5), NaCl (139), KCl (12), MgCl₂ (0.5), CaCl₂ (1.3), lactic acid,²¹ and pH 6.2 under 100% nitrogen ($\text{O}_2 < 1\%$) at 37°C for 8 hours.²² Reperfusion was initiated by changing cells to DMEM/M199 (4:1) supplemented with 2% (wt/vol) of FBS and continued for 16 hours in 95% air and 5% CO₂. Controls were incubated in control medium containing (in millimolar) HEPES, D-glucose (10), NaCl (139), KCl (4.7), MgCl₂ (0.5), CaCl₂ (1.3), and pH 7.4 in 95% air and 5% CO₂ and were reperfused as described in ischemic cells.

Measurement of Myocardial Function

Heart function was determined using Sonosite 180 plus echocardiograph equipped with an electronic 10-MHz linear array transducer. The following parameters were measured: Left ventricular end-systolic diameter (LVESD) and left ventricular end diastolic diameter (LVEDD). Fractional shortening percentage (FS) was calculated according to the formula $\text{FS} = [(\text{LVEDD} - \text{LVESD})/\text{left ventricular end-diastolic compliance}] \times 100 (\%)$.²³

Electron Microscopy

For the in vivo studies, the samples were obtained from the distal territory to the occlusion site of the anterior descending artery. In the case of peri-infarct region conditions, the tissue was collected proximally to artery occlusion. All samples correspond to the subendocardial muscle of the left ventricle and were fixed in 2% glutaraldehyde in 0.05 M (pH 7.3) cacodylate buffer, postfixed in 1% of OsO₄, dehydrated in ethanol, and embedded in Epon 812. Ultrathin sections were stained with aqueous uranyl acetate for 25 minutes and Reynolds lead citrate for 20 minutes and examined under a Philips Tecnai 12 BT electron microscope at 80 kV.²¹ In the case of cells, these were treated similarly but acquired on an FEI Tecnai G2 Spirit electron microscope equipped with a LaB6 source and operating at 120 kV. Measurements of mitochondrial area, circularity, and mitochondrial cristae-integrated density were made with the Multi Measure ROI tool of ImageJ.

Adenoviruses

The adenovirus expressing Drp1 dominant-negative K38A (Drp1K38A) was a gift of Dr Antonio Zorzano (IRB, Universitat of Barcelona, Spain). Cultured cardiomyocytes were transduced with Drp1K38A at a multiplicity of infection (MOI) of 2000 for 48 hours. Adenovirus encoding LacZ or GFP or empty vector (Mock) was used as a control. In vivo adenoviral infection of hearts was performed as described by Hajjar et al²⁴ Because Drp1K38A is not attached to any directly measurable protein, in vivo adenoviral infection was measured through the quantification of the associated fluorescence of hearts infected with an adenovirus of the same

family of the Drp1, coupled to a GFP protein. We assumed that the MOI of infection, in the case of a similar adenovirus, would be comparable.²⁵ After *in vivo* adenoviral infection, the fluorescence associated with the GFP adenovirus was 5–6 times higher than in control or sham rats (see **Figure 1, Supplemental Digital Content 1**, <http://links.lww.com/JCVP/A138>), whereas this same procedure increased Drp1 protein levels in the heart by about 235% for the case of Drp1K38A (Fig. 4A).

Subcellular Fractionation, Western Blot, and Immunohistochemistry

Protein extracts were prepared from cardiomyocytes as described.¹⁸ Heart subcellular fractions were obtained as described by Frezza et al.²⁶ Mitochondrial and cytosolic fractions were obtained by differential centrifugation of heart and cardiomyocyte homogenates. Tissues and cells were homogenized using a homogenizer with a tight-fitting Teflon pestle, pelleted and resuspended in ice-cold buffer containing 250 mM of sucrose, 1 mM of EGTA, and 10 mM of Hepes, pH 7.4; and the protease inhibitors PMSF, leupeptin, pepstatin A, and aprotinin. The homogenates were centrifuged ($\times 750g$, 10 minutes) to remove nuclei and unbroken cells, and supernatants were centrifuged ($\times 10,000g$, 25 minutes) to obtain a pellet highly enriched in mitochondria. The protein content was determined by Bradford's method. The purity of mitochondrial fraction, assessed by mtHsp70 levels, was at least 80% (see **Figure 2, Supplemental Digital Content 2**, <http://links.lww.com/JCVP/A139>).

Samples containing equal amounts of protein were then resolved by SDS-PAGE and electrotransferred to nitrocellulose (Bio-Rad Laboratories, Inc). Membranes were blocked in TBS 5% (wt/vol) milk and 0.1% (vol/vol) Tween 20 and probed with anti-Drp1 (BD Transduction Laboratories, San Jose, CA), Mfn2 (Abcam, Cambridge, MA), Fis1 and mtHsp70 (Alexis Biochemicals, San Diego, CA), β -actin and β -tubulin (Sigma Chemicals Co, St. Louis, MO). After secondary horseradish peroxidase-linked antibodies (Calbiochem), blots were developed by chemiluminescence using the ECL system (Perkin Elmer) and exposed to Kodak films. Bands were analyzed by scanning densitometry using the NIH software ImageJ. Immunohistochemistry was performed in cardiomyocytes cultured in gelatin-coated cover slips. Cells were fixed for 10 minutes with 4% of paraformaldehyde, permeabilized with 0.3% of Triton X-100 in phosphate-buffered saline, blocked for 1 hour with phosphate-buffered saline 5% bovine serum albumin (BSA), incubated overnight with anti-Drp1 (mouse 1:500) and Fis1 (rabbit 1:500), and revealed with Alexa 488 IgG rabbit and Alexa 565 IgG mouse antibodies. Cover slips were mounted in DakoCytomation fluorescent mounting medium (DakoCytomation). The resulting fluorescence was evaluated in a scanning Zeiss LSM-5, Pascal 5 Axiovert 200 confocal microscope, using the LSM 5 3.2 image capture and analysis software and a Plan-Apochromat 63x/1.4 Oil DIC objective.

Mitochondrial Dynamics

Cells were cultured on gelatin-coated cover slips and incubated with Mitotracker Green FM (400 nM) for 30 minutes

in Krebs solution. Confocal image stacks were captured with a Zeiss LSM-5, Pascal 5 Axiovert 200 microscope, using LSM 5 3.2 image capture and analysis software and a Plan-Apochromat 63x/1.4 Oil DIC objective. Images were deconvolved with the ImageJ software. Z-stacks were volume-reconstituted using the VolumeJ plug-in, the resulting images thresholded and changes in object (mitochondria), number, and volume quantified using the ImageJ-3D Object Counter plug-in. Each experiment was done at least 4 times, and 16–25 cells per condition were quantified. Fragmentation criteria were decrease in the mean individual mitochondrial volume and increase in total number of mitochondria.¹⁸

Immunofluorescence Studies and Colocalization Analysis of Drp1 and Fis1

These studies were performed as described above. For the colocalization analysis, only 1 focal plane was analyzed with a Zeiss LSM-5, Pascal 5 Axiovert 200 microscope. Images obtained were deconvolved, and background was subtracted using the ImageJ software. Colocalization between the proteins was quantified using the Pearson's and Manders' algorithm, as previously described.^{18,27,28}

Autophagy and Mitophagy Studies

Cells were cultured on gelatin-coated cover slips and stained with Mitotracker Orange FM (MTO; 400 nM) for 30 minutes in culture media. After that, the cells were prepared for immunofluorescence as described above. An anti-LC3 antibody (1:100) was used as a marker of autophagy. One focal plane was obtained with a Zeiss LSM-5, Pascal 5 Axiovert 200 microscope. The images obtained were deconvolved, thresholded, and used for particle analysis with the ImageJ software. Elements bigger than 10 pixels² were considered as autophagosomes, and cells showing more than 3 autophagosomes were counted as autophagic. The percentage of cells with autophagic phenotype was determined. Additionally, a colocalization analysis was performed with the MTO and LC3 signals to determine changes in mitophagy. The Manders' coefficient was determined as a measure of colocalization.^{18,27,28}

Mitochondrial Function

Mitochondrial membrane potential was measured as described previously.²⁹ Briefly, cells were loaded with 200 nM tetramethylrhodamine methyl ester (Molecular Probes, used in nonquenching mode) for 30 minutes at 37°C. Then, cells were trypsinized, and cell fluorescence was determined by flow cytometry ($\lambda_{excitation} = 543 \text{ nm}$; $\lambda_{emission} = 560 \text{ nm}$) using a FAC Scan system (Becton Dickinson, San Jose, CA). Carbonyl cyanide 3-chlorophenylhydrazone (CCCP) of 50 μM for 30 minutes was used as positive control of mitochondrial depolarization.²⁹ Data were expressed as percentage of fluorescence intensity relative to control fluorescence. Oxygen consumption rate (OCR) was measured in suspended cells in an isolated chamber at 25°C, coupled to a Clark electrode 5331 (Yellow Springs Instruments). Maximal respiration was obtained using CCCP (10 μM), whereas proton leak was obtained using oligomycin (10 μM). Intracellular ATP

levels were determined using luciferin/luciferase assay (Cell-Titer Glo Kit; Promega) as described previously.²⁹ Cell viability was determined by flow cytometry and propidium iodide as previously described.¹⁹

Statistical Analysis

Data are presented either as mean \pm SEM of a number (n) of independent experiments or as examples of representative experiments performed on at least 3 separate occasions. Data were analyzed using analysis of variance; comparisons between groups were performed using a protected Tukey's *t* test or 2-way analysis of variance. A value of $P < 0.05$ was chosen as the limit of statistical significance.

RESULTS

I/R Induces Mitochondrial Remodeling in the Heart

To evaluate the effects of I/R on the mitochondrial network *in vivo*, we studied mitochondrial morphology in rat hearts subjected to a left anterior descending coronary artery ligation for 30 minutes, followed by 150 minutes of reperfusion. We found that I/R impaired cardiac function (see **Figure 2A**, **Supplemental Digital Content 2**, <http://links.lww.com/JCVP/A139> and Table 1) and increased CK-MB plasma levels (see **Figure 2B**, **Supplemental Digital Content 2**, <http://links.lww.com/JCVP/A139>) and myocardial infarction size (see **Figure 2C**, **Supplemental Digital Content 2**, <http://links.lww.com/JCVP/A139>). Figure 1A shows electronic microscope images for infarcted and sham rats. The first ones presented an increase in mitochondrial electron density, myofibrillar disorganization, and abundant perimitochondrial debris compared with sham rats. To determine whether I/R-induced changes in mitochondrial dynamics-related proteins, subcellular fractionation was performed. We obtained cytosolic and mitochondrial fractions with purities of $>85\%$ and $>80\%$, respectively (see **Figure 3**, **Supplemental Digital Content 3**, <http://links.lww.com/JCVP/A140>). Mfn2 levels were significantly decreased in the infarcted region as compared with peri-infarcted region (see **Figure 4**, **Supplemental Digital Content 4**, <http://links.lww.com/JCVP/A141>). As expected, Mfn2 was not detected in cytoplasmic fractions. In contrast, Drp1 mitochondrial levels

were not modified by I/R (Fig. 1C). Cytosolic levels of Drp1 were not observed in Figure 1C because of the low exposition of films. To test whether I/R modifies Drp1 subcellular distribution, mitochondrial/cytosolic Drp1 ratio was determined and higher exposition of films were used. I/R increased mitochondrial/cytosolic Drp1 ratio in both risk and infarcted regions as compared with ischemic sham rats (17.8 ± 4.2 and 19.8 ± 5.1 fold, respectively, $P < 0.01$) (Fig. 1D). The results obtained show that I/R stimulate translocation of Drp1 and decreased of Mfn2 levels suggesting the induction of mitochondrial fission.

Drp1 Inhibition Protects Heart Subjected to I/R

To determine the role of Drp1 on I/R injury, we performed a cardiac adenoviral delivery of Drp1K38A, a dominant-negative form of Drp1. Drp1K38A-treated hearts showed a significant increase in Drp1 protein levels as compared with a GFP-encoding adenovirus (Fig. 2A). Myocardial infarct size induced by I/R was significantly smaller in Drp1K38A than GFP-overexpressing hearts (in percentage) (28 ± 3 vs. 15 ± 2 , $P < 0.05$) (Fig. 2B). Drp1K38A-treated rats also showed improved myocardial function after I/R. Echocardiography showed that rats transduced with the Drp1K38A adenovirus had a FS of 46%, which is significantly greater than the 30% of adenovirus-GFP-treated rats ($P < 0.05$) (Fig. 2C and Table 1). Altogether, these data suggest a protective role of Drp1 inhibition against I/R injury.

Drp1 Inhibition Exerts Cardioprotection on Cultured Cardiomyocytes Exposed to I/R Injury

Exposure of cultured cardiomyocytes to simulated I/R induced a morphological change from tubular to spherical or fragmented mitochondria (Fig. 3A). To assess mitochondrial network integrity, we performed a 3D-reconstitution of the mitochondrial network. Both the number of mitochondria per cell and the average volume of each mitochondrion were determined as described in Methods. As compared with control cells, cardiomyocytes exposed to I/R showed a significant increase in the number of mitochondria (from 283 ± 40 to 1183 ± 469 , $P < 0.05$) with a reduction in mitochondrial volume (from 1120 ± 420 to 180 ± 30 , $P < 0.05$). To examine detailed changes in mitochondrion morphology in response to I/R, we also performed electron microscopy analysis. The data showed a significant I/R-dependent decrease in the number of large mitochondria and the appearance of active fission sites highlighted with black arrows (Fig. 3B). In addition, I/R decreased mitochondrion size (-33%) and increased the circularity index (from 0.70 ± 0.25 to 0.82 ± 0.05). Furthermore, I/R decreased the percentage of cells displaying a dense cristae structure (41%), which was also corroborated by the parameter of integrated density for this organelle (Fig. 3C).

Furthermore, to assess the involvement of mitochondrial fission machinery in the observed fragmentation, we performed indirect immunofluorescence for Drp1 and Fis1. Drp1 translocation from the cytosol to mitochondria is the

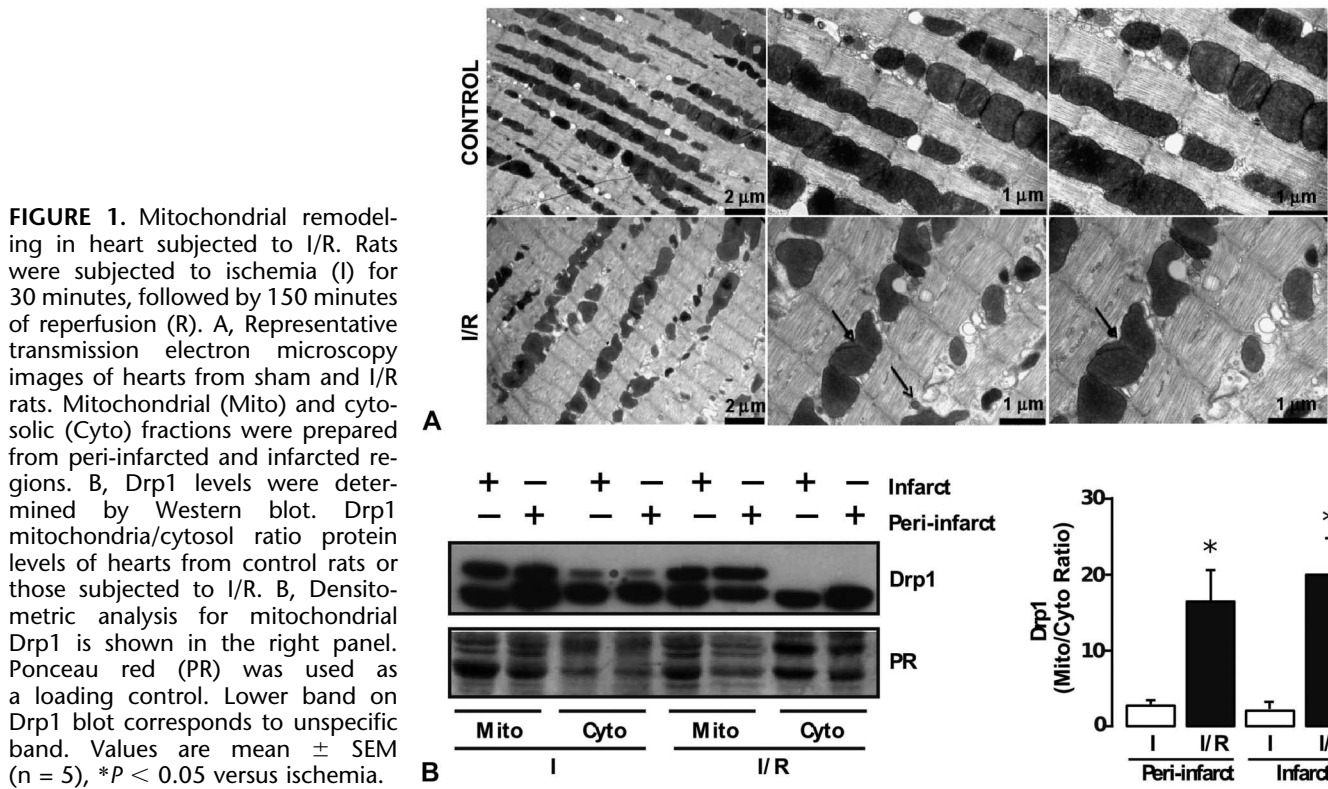
TABLE 1. Protective Role of Drp1 Loss-of-function on Cardiac Parameters in I/R Injury

	Control	I/R	
		GFP	Drp1K38A
Body weight, g	229 \pm 7	225 \pm 30	248 \pm 35
LVEDD, mm	58 \pm 3	63 \pm 2	56 \pm 8
LVESD, mm	28 \pm 2	44 \pm 8	30 \pm 5*
FS, %	52 \pm 4	30 \pm 3	46 \pm 2*

Data are mean \pm SEM.

* $P < 0.05$ versus GFP.

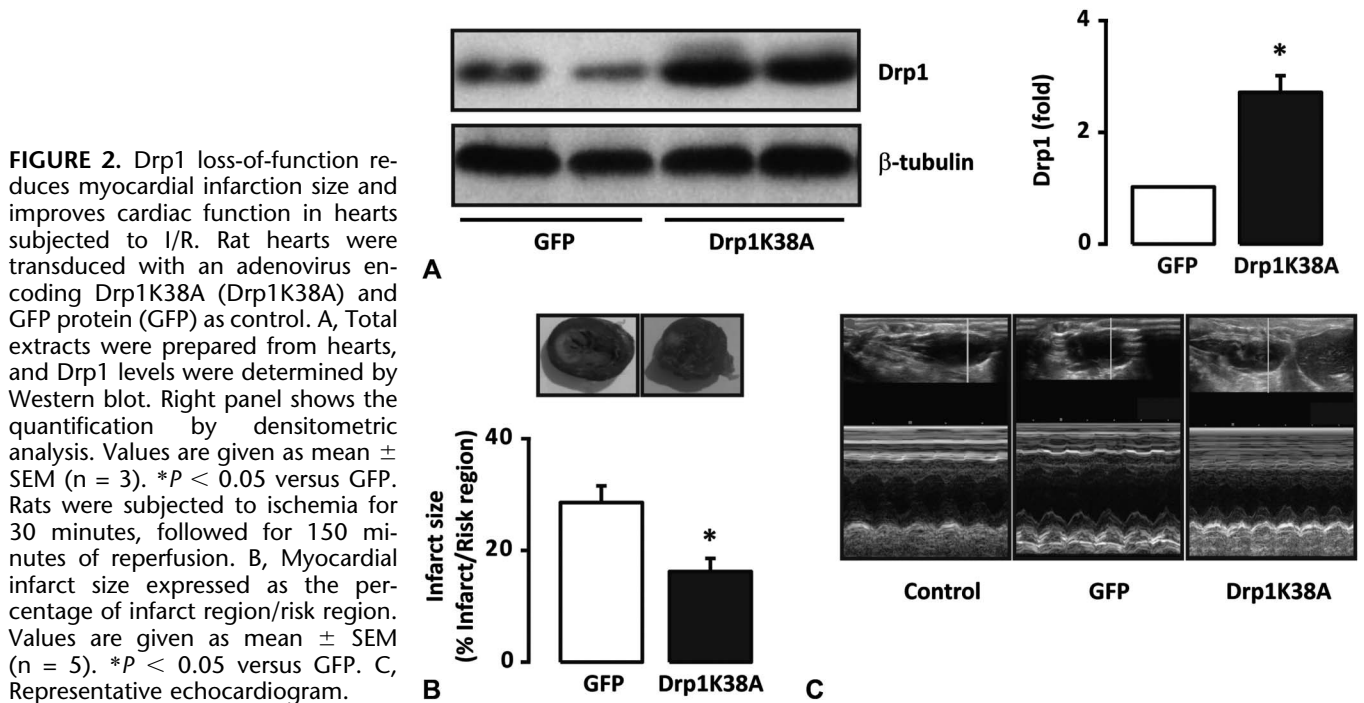
GFP, transduced with adenovirus encoding GFP; Drp1K38A, transduced with adenovirus encoding dominant-negative Drp1K38A.



first step of mitochondrial fission.⁹ Accordingly, I/R induced a significant increase in the Pearson's and Manders' colocalization indexes of both proteins (Fig. 3B) (*P* < 0.05).

To further explore the role of Drp1 loss-of-function, cultured cardiomyocytes were transduced with Drp1K38A.

These cells showed a 9-fold increase in Drp1 levels over control (mock adenovirus) (Fig. 4A). Drp1K38A induced a significant decrease in the number of mitochondria per cell (from 220 ± 25 to 105 ± 10 , *P* < 0.05) and increased mitochondrial volume (from 1850 ± 120 to 4060 ± 450 ,



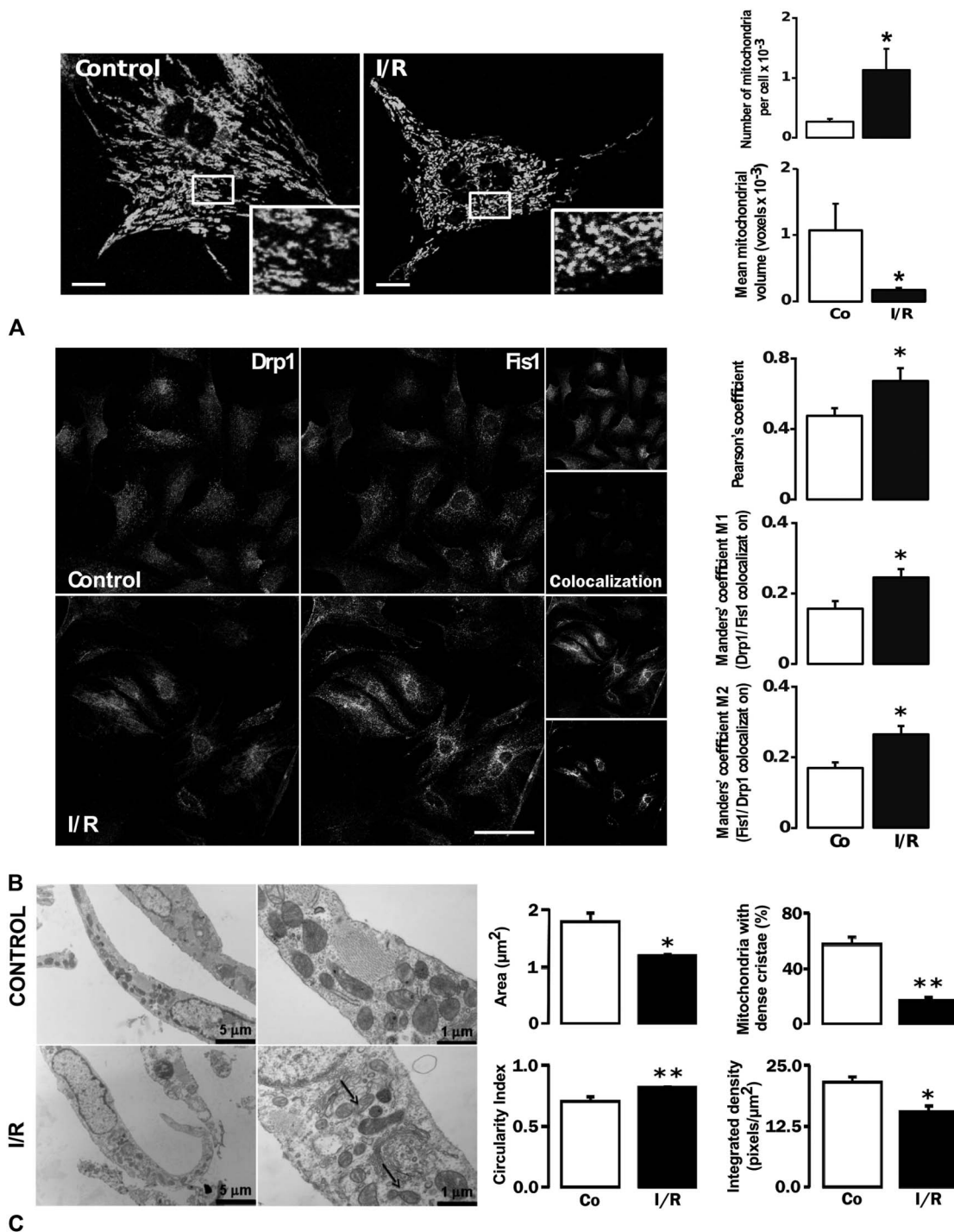


FIGURE 3. Simulated I/R induces mitochondrial fission in cultured cardiomyocytes. Cells were exposed to control (Co) or simulated I/R. **A**, Multislice imaging reconstitutions of cardiomyocytes loaded with MitoTracker green were obtained by confocal microscopy to show mitochondrial morphology. The mean mitochondrial volume and the number of mitochondria per cell were determined. The scale bar is 10 μm. Values are given as mean ± SEM (n = 5), *P < 0.05 versus control. **B**, Cells were stained with Alexa antibodies for Drp1 (green) or Fis1 (red) to determine colocalization. The mean level of Drp1 and Fis1 colocalization was determined by Pearson's correlation (top panel), Manders' coefficient M1 (Drp1 to Fis1 colocalization) (middle panel), and Manders' coefficient M2 (Fis1 to Drp1 colocalization) (lower panel). The scale bar is 20 μm. Values are given as mean ± SEM (n = 5), *P < 0.05 versus control. **C**, Representative transmission electron microscopy images from controls and cells submitted to I/R. Two different magnifications of the same cell are shown. Arrows indicate fission active sites. Mitochondrial area (upper left), circularity index (lower left), percentage of mitochondria with dense cristae (upper right), and cristae-integrated density (lower right) were quantified. Data are from 100 mitochondria per condition from 3 separate experiments. Data are mean ± SEM (n = 3). *P < 0.05 and **P < 0.01 versus control.

$P < 0.05$) (Fig. 4B). To assess the protective role of Drp1 inhibition against I/R-induced cell death, we subjected Drp1K38A-transduced cardiomyocytes to simulated I/R, and cell viability was determined by propidium iodide incorporation and flow cytometry. Drp1K38A induced a 40% reduction of cell death as compared with mock adenovirus (Fig. 4C).

Drp1 Loss-of-function Induces Metabolic Changes in Cultured Neonatal Cardiomyocytes Subjected to I/R

Given the morphological and functional changes observed with the Drp1K38A adenovirus and to further elucidate whether the protective role of mitochondrial fusion in I/R injury was linked to changes in mitochondrial function, metabolic parameters including mitochondrial membrane potential ($\Delta\Psi_m$), intracellular ATP levels, and OCRs were measured in cultured cardiomyocytes. Drp1K38A-transduced cells showed a lower $\Delta\Psi_m$ (from 1.0 to 0.6, $P < 0.05$) as compared with those transduced with LacZ. However, when both LacZ- and Drp1K38A-transduced cardiomyocytes were submitted to I/R, $\Delta\Psi_m$ was reduced in both cases (from 1.0 to 0.2, $P < 0.05$ and from 0.6 to 0.2, $P < 0.05$, transduced with LacZ and Drp1K38A, respectively) (Fig. 5A). No reduction in basal ATP levels were observed in Drp1K38A-overexpressing cells as compared with LacZ. In fact, Drp1K38A increased ATP levels when compared with controls. However, on I/R, cardiomyocytes-overexpressing Drp1K38A showed a less dramatic ATP level reduction as compared with LacZ cells (0.55 ± 0.06 fold reduction vs. 0.80 ± 0.02 fold reduction in LacZ and Drp1K38A-overexpressing cardiomyocytes, respectively) (Fig. 5B).

OCR was significantly lower in Drp1K38A cells as compared with LacZ cells (from 100 to 53 ± 3 , $P < 0.05$) (Fig. 5C). Maximal OCR was also greatly reduced (from 159 ± 19 to 73 ± 5 , $P < 0.05$), suggesting that oxidative phosphorylation is compromised in Drp1K38A-transduced cardiomyocytes (Fig. 5D). I/R reduced both basal and maximal OCR to a greater extent in Drp1K38A than LacZ-treated cells (74 ± 11 fold reduction vs. 20 ± 4 fold reduction in LacZ and Drp1K38A-overexpressing cardiomyocytes, respectively) (Fig. 5C). Interestingly, respiration rates in the presence of oligomycin, a direct measure of the proton leak rate across the mitochondrial membrane, were consistently higher in cells transduced with the Drp1K38A adenovirus (from 37 ± 5 to 50 ± 3 , $P < 0.05$), a difference that was even greater in the I/R cardiomyocytes (41 ± 5 to 56 ± 5 , $P < 0.05$) (Fig. 5E).

In summary, these data show that Drp1K38A-transduced cardiomyocytes have a decreased OCR with no reduction in intracellular ATP level and a larger decrease in OCR with a smaller reduction in intracellular ATP level on I/R, when compared with controls. These results suggest that cardioprotection against I/R injury induced by Drp1K38A could be explained by a reduced oxygen dependence of ATP production in the transduced cardiomyocytes. Moreover, given that the state 4 condition respiration rate (oligomycin-treated cells) is strongly

controlled by proton leak kinetics and partially by substrate oxidation,³⁰ the protection exerted by the Drp1K38A adenovirus could be related to an unexpected mitochondrial uncoupling process, mainly related to diminished mitochondrial ROS production induced by I/R and a metabolic switch to less oxidative forms of energy production.

DISCUSSION

In this study, we report that Drp1 loss-of-function, by overexpression of its dominant-negative form Drp1K38A, leads to cardioprotection in the onset of I/R through a decreased oxygen-dependent metabolism characterized by a reduction on OCR and $\Delta\Psi_m$ with no changes in intracellular levels of ATP related to an increase on mitochondrial fusion. Several studies reported that cells depleted of Drp1 consume less oxygen,^{31,32} thus supporting some of our conclusions. Recently, Hong et al identified a critical role for Drp1-mediated mitochondrial fission in the oxygen-induced closure of ductus arteriosus. Oxygen induces fission through the phosphorylation of Drp1 and an increase in OCR, whereas Drp1 inhibition blocks oxygen-mediated ductus arteriosus closure.³³

Mitochondrial dynamics has been shown to play a critical role in determining mitochondrial morphology and function. Furthermore, we know that a continuous balance between mitochondrial fission and fusion is critical for maintaining proper mitochondrial function. However, in cardiomyocytes, this important issue has only recently begun to be addressed, possibly because of the general perception that the highly structured organization of adult ventricular cardiomyocytes prevents mitochondrial dynamics from playing a relevant role. Interestingly, cardiac tissue contains higher levels of many of the proteins involved in mitochondrial dynamics than other tissues.^{9,10} We show that overexpression of Drp1K38A induces cardioprotection on I/R both in vitro and in vivo. Cardioprotection observed in Drp1K38A-transduced cells could be due to a lower dependence on mitochondrial oxidative phosphorylation for ATP generation and a metabolic switch.

Mitochondrial fission accompanies most forms of cell death, whereas mitochondrial fusion induces protection from apoptosis.³⁴ Earlier studies using electron microscopy revealed that mitochondria become fragmented after induction of cell death by different stimuli.^{35,36} Recent studies using time-lapse microscopy revealed that mitochondrial fission coincided very closely with the induction of cell death. Fission was observed at the same time as Bax activation in the mitochondria, but before mitochondrial outer membrane permeabilization and cytochrome c release.³⁷ Several studies of multiple apoptotic systems suggest causal links among mitochondrial fission, the execution of cell death, and both mitochondrial fission factors Fis1 and Drp1.¹⁰ During apoptosis, mitochondria undergo rapid fragmentation, a process dependent on the translocation of cytosolic Drp1 to mitochondria.³⁸ We have found consistently increased colocalization of Drp1 with Fis1 after I/R injury and increased Drp1 translocation to the mitochondria. Moreover, we also found that I/R decreases Mfn2 levels in rat hearts, similar to what others have found in brain and kidney.^{39,40}

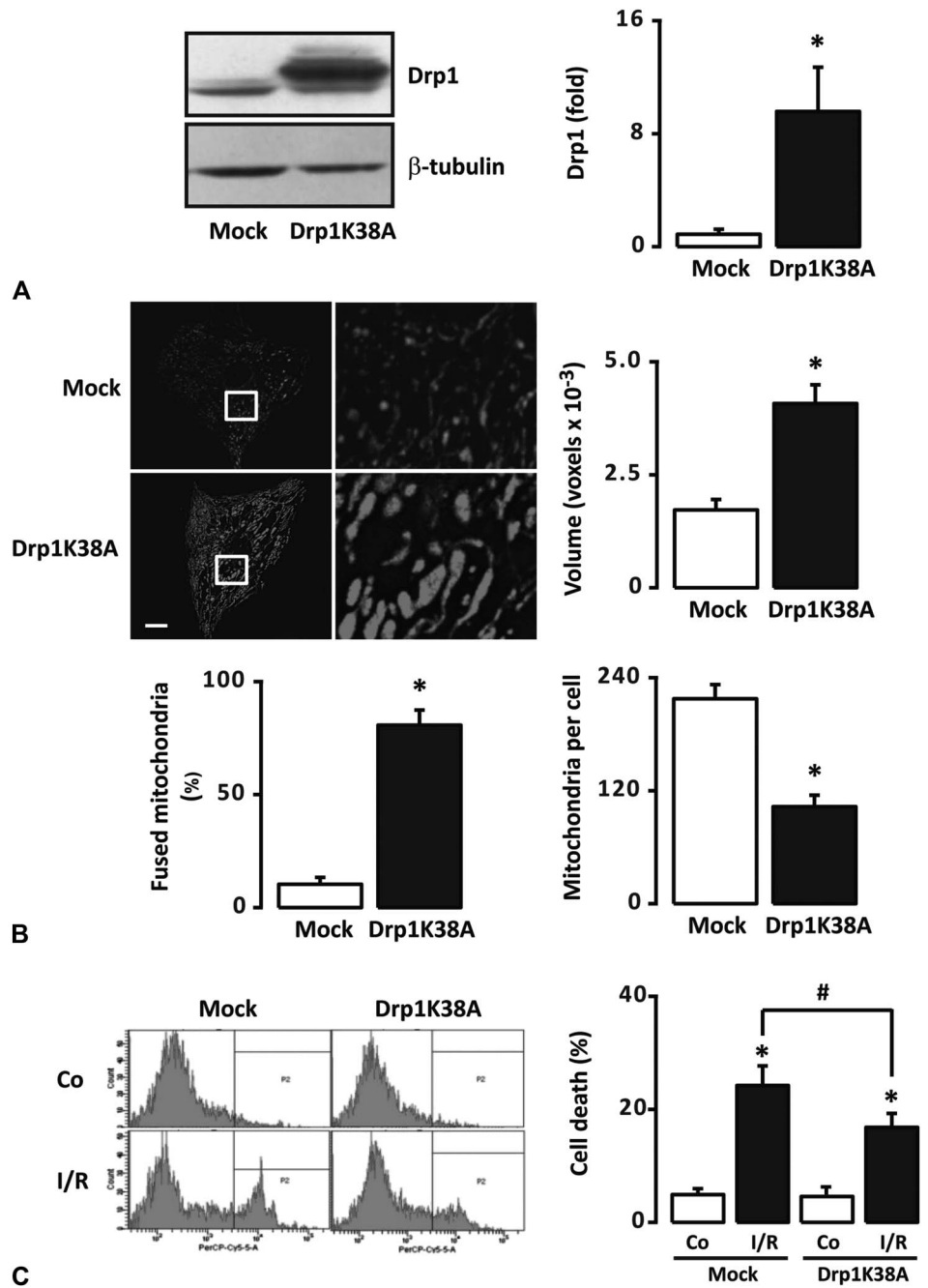


FIGURE 4. Drp1 loss-of-function protects from I/R-induced cell death in vitro. Cultured cardiomyocytes were transduced for 48 hours with adenovirus encoding Drp1K38A protein (MOI = 1000) or empty adenovirus as mock (MOI = 1000) as control. **A**, Western blot (left panel) and densitometric analysis (right panel) of Drp1. **B**, Analysis of mitochondrial dynamics was performed as described in Figure 1. Images were used to evaluate the mitochondrial volume (upper right panel), cells with fused mitochondria (lower left panel), and mitochondrial number (lower right panel). The scale bar is 10 μ m. Values are mean \pm SEM (n = 3). **P* < 0.05 versus mock. **C**, Cell death was determined in PI permeable cells by flow cytometry. Cells were transduced with Drp1K38A or mock and subjected to I/R. Representative histogram (left panel) and cell death quantification (right panel). Values are given as mean \pm SEM (n = 4). **P* < 0.05 versus mock. #*P* < 0.05 versus I/R mock.

Drp1K38A-transfected cardiomyocytes exhibited an extensive and elongated mitochondrial network. This phenotype persisted even when these cardiomyocytes were exposed to I/R. This particular configuration was previously associated with a reduction in sensitivity to apoptosis stimuli.¹⁵ In the kidney, I/R injury has been reported to occur through the induction of Drp1-dependent mitochondrial fragmentation and apoptosis, and prevention of this process was found to be beneficial.⁴¹ The beneficial effect of mitochondrial network modification on cardiac I/R injury was first demonstrated by Ong et al¹⁷ This group showed that in vivo pharmacological treatment with the Drp1 inhibitor mdivi-1

significantly increased the proportion of elongated interfibrillar mitochondria in the ischemic adult murine heart and protected adult cardiomyocytes from I/R by reducing myocardial infarct size. This cardioprotective effect was elicited by mitochondrial elongation first linked to the inhibition of mPTP opening. Recently, Chanoit et al⁴² showed that inhibition of phosphodiesterase prevents MPTP opening by PKA-dependent mechanisms in H9c2 cells. Other reports have shown that inhibition of phosphodiesterase III protects from I/R injury by increasing cAMP levels and activating PKA.^{43–45} Moreover, the cAMP-PKA pathway induces mitochondrial elongation through inhibition of Drp1.⁴⁶ However, the specific

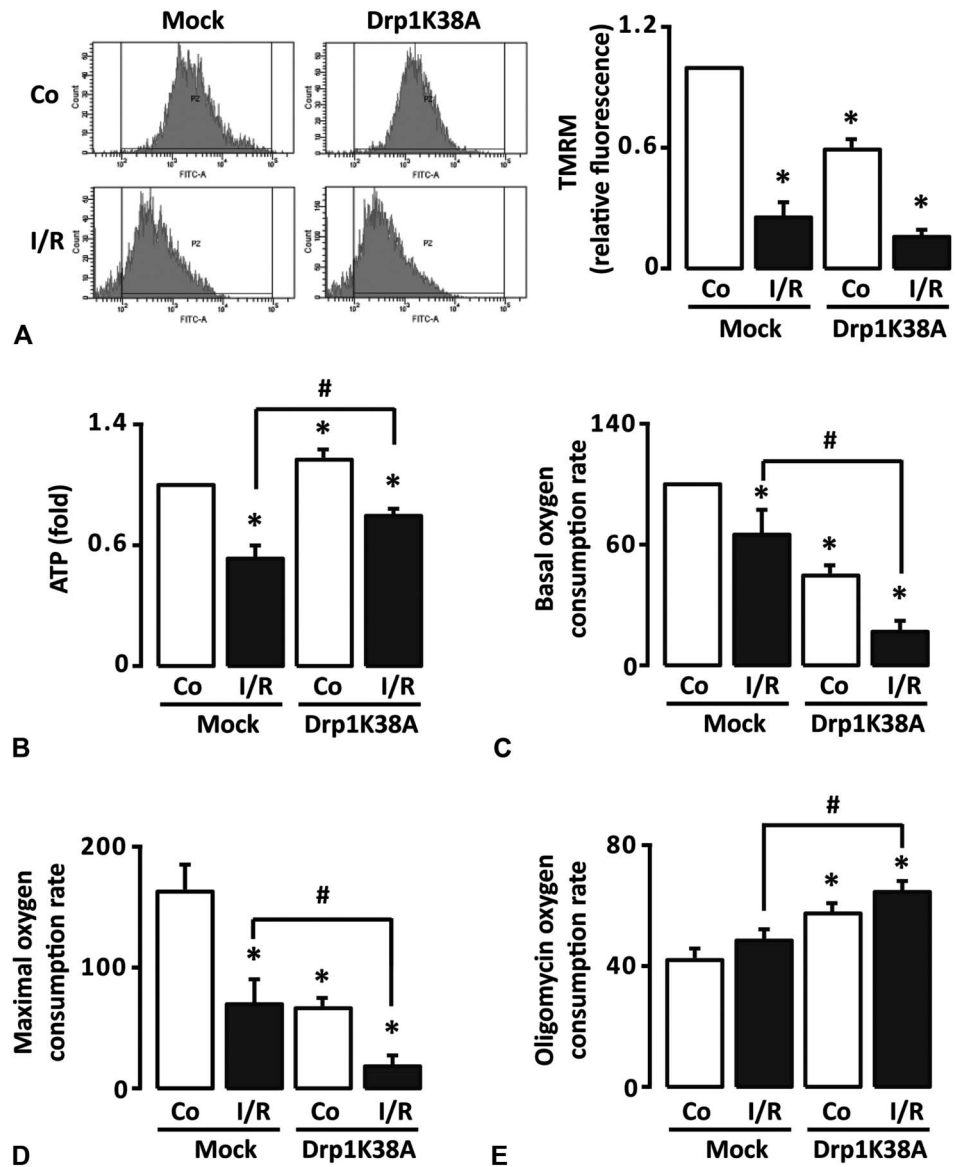


FIGURE 5. Drp1 loss-of-function induces metabolic adaptive responses in cultured cardiomyocytes. Cells were transfected for 48 hours with adenovirus encoding the Drp1K38A protein (MOI = 1000) or empty adenovirus as mock (MOI = 1000). Transduced cardiomyocytes were subjected to ischemia (30 minutes) and reperfusion (150 minutes) (I/R) or control (Co). A, Determination of $\Delta\Psi_m$ in tetramethylrhodamine methyl ester-stained cells. B, Quantification of intracellular ATP levels. C, Basal, (D) maximal, and (E) oligomycin-dependent oxygen (proton leak) consumption in cultured cardiomyocytes. Values are given as mean \pm SEM (n = 5). **P* < 0.05 versus control mock; #*P* < 0.05 versus I/R mock.

mechanism through which the inhibition of Drp1 function prevents mPTP opening remains unknown.

In our model, we observed a protective effect both in vivo and in vitro on I/R through the inhibition of Drp1 function by overexpression of its dominant-negative form, Drp1K38A. Given the critical role of mitochondria in the citric acid cycle, the electron transport chain, oxidative phosphorylation, fatty acid oxidation, and amino acid catabolism, it is not surprising that alterations of mitochondrial function could exert a dramatic effect on cell survival. Our results show that the protective effect of the adenovirus Drp1K38A is mediated by mitochondrial metabolic changes. Drp1K38A-transfected cells showed a strong inhibition of $\Delta\Psi_m$ and OCR without affecting intracellular ATP. After I/R, Drp1K38A-transfected cells had even lower levels of $\Delta\Psi_m$ and OCR, but the ATP drop in these cells was partially inhibited. These results show that inhibition of Drp1 depressed

mitochondrial respiration, possibly by blocking electron transport and/or increasing uncoupled respiration, leading to a metabolic switch that makes cardiomyocytes less dependent on oxidative phosphorylation for ATP production. This idea is further reinforced by the OCRs obtained in the presence of oligomycin, which were higher in Drp1K38A-treated cells than controls, suggesting an uncoupling of the mitochondrial network due to changes in the proton leak or $\Delta\Psi_m$ caused by altered substrate oxidation.³⁰

Blockage of electron transport and partial uncoupling of respiration are 2 mechanisms known to decrease cardiac injury after I/R.⁴⁷ Although protection by inhibition of electron transport or uncoupling of respiration initially seems counterintuitive, the continuation of mitochondrial oxidative phosphorylation in the pathological milieu of ischemia generates reactive oxygen species, mitochondrial calcium overload, and cytochrome c release. Surprisingly, a substantial

portion of the damage to the mitochondrial electron transport chain and to oxidative phosphorylation occurs during ischemia, rather than reperfusion.⁴⁸ Ischemic mitochondrial damage seems to be a major mechanism of cardiac injury because reperfusion of myocardium with healthy and preserved mitochondria suffers markedly less myocardial injury. During reperfusion, ischemia-damaged mitochondria produce even more oxidative damage, cause calcium-driven cardiomyocyte injury, and lead to a greater activation of apoptotic pathways. Paradoxically, transient inhibition of mitochondrial activity by ischemia, hypoxia, or pharmacological inhibition during early reperfusion decreases myocardial injury, presumably by blunting the deleterious consequences of respiration by damaged mitochondria.⁴⁹ Thus, the restriction of mitochondrial oxidative metabolism by therapeutic intervention through the activation of signaling cascades is a key mechanism of cardiac protection during I/R. Moreover, uncoupling of mitochondria, mainly through increases in the uncoupling protein 2, is thought to protect cardiomyocytes against oxidative stress by dissipating the mitochondrial proton gradient and $\Delta\Psi_m$, thereby reducing ROS generation.^{50,51} However, the relationship of this process with mitochondrial fission and the Drp1 protein requires additional study.

CONCLUSIONS

Adenoviral overexpression of a dominant-negative Drp1K38A in vivo and in vitro induced cardioprotection against the injury triggered by I/R. The cardioprotective mechanism involved the decrease in the oxygen-dependent metabolism characterized by a reduction on OCR and $\Delta\Psi_m$ with no changes in intracellular levels of ATP. These results may further add to the evidence that manipulation of mitochondrial dynamics during I/R could be used as a procedure to induce cardioprotection.

ACKNOWLEDGMENTS

The authors thank Dr. Antonio Zorzano (Institute of Research in Biomedicine, Barcelona, Spain) for his kind donation of Drp1K38A adenovirus. They also thank José López, Alejandro Correa, and Fidel Albornoz for their excellent technical assistance.

REFERENCES

- Thygesen K, Alpert JS, White HD, et al. Universal definition of myocardial infarction. *Circulation*. 2007;116:2634–2653.
- Thygesen K, Alpert JS, Jaffe AS, et al. Diagnostic application of the universal definition of myocardial infarction in the intensive care unit. *Curr Opin Crit Care*. 2008;14:543–548.
- Kuzmicic J, Del Campo A, Lopez-Crisosto C, et al. Mitochondrial dynamics: a potential new therapeutic target for heart failure. *Rev Esp Cardiol*. 2011;64:916–923.
- Huss JM, Kelly DP. Mitochondrial energy metabolism in heart failure: a question of balance. *J Clin Invest*. 2005;115:547–555.
- Neubauer S. The failing heart—an engine out of fuel. *N Engl J Med*. 2007;356:1140–1151.
- Buchwald A, Till H, Unterberg C, et al. Alterations of the mitochondrial respiratory chain in human dilated cardiomyopathy. *Eur Heart J*. 1990;11:509–516.
- Graham BH, Waymire KG, Cottrell B, et al. A mouse model for mitochondrial myopathy and cardiomyopathy resulting from a deficiency in the heart/muscle isoform of the adenine nucleotide translocator. *Nat Genet*. 1997;16:226–234.
- Stojanovski D, Koutsopoulos OS, Okamoto K, et al. Levels of human Fis1 at the mitochondrial outer membrane regulate mitochondrial morphology. *J Cell Sci*. 2004;117:1201–1210.
- Parra V, Verdejo H, del Campo A, et al. The complex interplay between mitochondrial dynamics and cardiac metabolism. *J Bioenerg Biomembr*. 2011;43:47–51.
- Chen H, Chan DC. Emerging functions of mammalian mitochondrial fusion and fission. *Hum Mol Genet*. 2005;14:R283–R289.
- Rojo M, Legros F, Chateau D, et al. Membrane topology and mitochondrial targeting of mitofusins, ubiquitous mammalian homologs of the transmembrane GTPase Fzo. *J Cell Sci*. 2002;115:1663–1674.
- Santel A, Fuller MT. Control of mitochondrial morphology by a human mitofusin. *J Cell Sci*. 2001;114:867–874.
- Cipolat S, Martins de Brito O, Dal Zilio B, et al. OPA1 requires mitofusin 1 to promote mitochondrial fusion. *Proc Natl Acad Sci U S A*. 2004;101:15927–15932.
- Satoh M, Hamamoto T, Seo N, et al. Differential sublocalization of the dynamin-related protein OPA1 isoforms in mitochondria. *Biochem Biophys Res Commun*. 2003;300:482–493.
- Lee YJ, Jeong SY, Karbowski M, et al. Roles of the mammalian mitochondrial fission and fusion mediators Fis1, Drp1, and Opa1 in apoptosis. *Mol Biol Cell*. 2004;15:5001–5011.
- Kanzaki Y, Terasaki F, Okabe M, et al. Giant mitochondria in the myocardium of a patient with mitochondrial cardiomyopathy: transmission and 3-dimensional scanning electron microscopy. *Circulation*. 2010;121:831–832.
- Ong SB, Subrayan S, Lim SY, et al. Inhibiting mitochondrial fission protects the heart against ischemia/reperfusion injury. *Circulation*. 2010;121:2012–2022.
- Parra V, Eisner V, Chiong M, et al. Changes in mitochondrial dynamics during ceramide-induced cardiomyocyte early apoptosis. *Cardiovasc Res*. 2008;77:387–397.
- Chen J, Chemaly E, Liang L, et al. Effects of CXCR4 gene transfer on cardiac function after ischemia-reperfusion injury. *Am J Pathol*. 2010;176:1705–1715.
- Domenech RJ, Macho P, Velez D, et al. Tachycardia preconditions infarct size in dogs: role of adenosine and protein kinase C. *Circulation*. 1998;97:786–794.
- Mariscalco G, Engstrom KG, Ferrarese S, et al. Relationship between atrial histopathology and atrial fibrillation after coronary bypass surgery. *J Thorac Cardiovasc Surg*. 2006;131:1364–1372.
- Pedrozo Z, Sanchez G, Torrealba N, et al. Calpains and proteasomes mediate degradation of ryanodine receptors in a model of cardiac ischemic reperfusion. *Biochim Biophys Acta*. 2010;1802:356–362.
- Ronco AM, Montenegro M, Castillo P, et al. Maternal exposure to cadmium during gestation perturbs the vascular system of the adult rat offspring. *Toxicol Appl Pharmacol*. 2011;251:137–145.
- Hajjar RJ, Schmidt U, Matsui T, et al. Modulation of ventricular function through gene transfer in vivo. *Proc Natl Acad Sci U S A*. 1998;95:5251–5256.
- Mittereder N, March KL, Trapnell BC. Evaluation of the concentration and bioactivity of adenovirus vectors for gene therapy. *J Virol*. 1996;70:7498–7509.
- Frezza C, Cipolat S, Scorrano L. Organelle isolation: functional mitochondria from mouse liver, muscle and cultured fibroblasts. *Nat Protoc*. 2007;2:287–295.
- Costes SV, Daelemans D, Cho EH, et al. Automatic and quantitative measurement of protein-protein colocalization in live cells. *Biophys J*. 2004;86:3993–4003.
- Ramirez O, Garcia A, Rojas R, et al. Confined displacement algorithm determines true and random colocalization in fluorescence microscopy. *J Microsc*. 2010;239:173–183.
- Bravo R, Vicencio JM, Parra V, et al. Increased ER-mitochondrial coupling promotes mitochondrial respiration and bioenergetics during early phases of ER stress. *J Cell Sci*. 2011;124:2143–2152.
- Brand MD, Nicholls DG. Assessing mitochondrial dysfunction in cells. *Biochem J*. 2011;435:297–312.
- Estaquier J, Arnoult D. Inhibiting Drp1-mediated mitochondrial fission selectively prevents the release of cytochrome c during apoptosis. *Cell Death Differ*. 2007;14:1086–1094.

32. Benard G, Bellance N, James D, et al. Mitochondrial bioenergetics and structural network organization. *J Cell Sci.* 2007;120:838–848.
33. Hong Z, Kutty S, Toth PT, et al. Role of dynamin-related protein 1 (drp1)-mediated mitochondrial fission in oxygen sensing and constriction of the ductus arteriosus. *Circ Res.* 2013;112:802–815.
34. Karbowski M. Mitochondria on guard: role of mitochondrial fusion and fission in the regulation of apoptosis. *Adv Exp Med Biol.* 2010;687:131–142.
35. Martinou I, Desagher S, Eskes R, et al. The release of cytochrome c from mitochondria during apoptosis of NGF-deprived sympathetic neurons is a reversible event. *J Cell Biol.* 1999;144:883–889.
36. Sheridan JW, Bishop CJ, Simmons RJ. Biophysical and morphological correlates of kinetic change and death in a starved human melanoma cell line. *J Cell Sci.* 1981;49:119–137.
37. Martinou JC, Youle RJ. Which came first, the cytochrome c release or the mitochondrial fission? *Cell Death Differ.* 2006;13:1291–1295.
38. Youle RJ, Karbowski M. Mitochondrial fission in apoptosis. *Nat Rev Mol Cell Biol.* 2005;6:657–663.
39. Funk JA, Schnellmann RG. Accelerated recovery of renal mitochondrial and tubule homeostasis with SIRT1/PGC-1 α activation following ischemia-reperfusion injury. *Toxicol Appl Pharmacol.* 2013;273:345–354.
40. Kumari S, Anderson L, Farmer S, et al. Hyperglycemia alters mitochondrial fission and fusion proteins in mice subjected to cerebral ischemia and reperfusion. *Transl Stroke Res.* 2012;3:296–304.
41. Brooks C, Wei Q, Cho SG, et al. Regulation of mitochondrial dynamics in acute kidney injury in cell culture and rodent models. *J Clin Invest.* 2009;119:1275–1285.
42. Chanoit G, Zhou J, Lee S, et al. Inhibition of phosphodiesterases leads to prevention of the mitochondrial permeability transition pore opening and reperfusion injury in cardiac H9c2 cells. *Cardiovasc Drugs Ther.* 2011;25:299–306.
43. Sanada S, Kitakaze M, Papst PJ, et al. Cardioprotective effect afforded by transient exposure to phosphodiesterase III inhibitors: the role of protein kinase A and p38 mitogen-activated protein kinase. *Circulation.* 2001;104:705–710.
44. Lochner A, Genade S, Tromp E, et al. Role of cyclic nucleotide phosphodiesterases in ischemic preconditioning. *Mol Cell Biochem.* 1998;186:169–175.
45. Rechtman MP, Van der Zyppe A, Majewski H. Amrinone reduces ischaemia-reperfusion injury in rat heart. *Eur J Pharmacol.* 2000;402:255–262.
46. Chang CR, Blackstone C. Cyclic AMP-dependent protein kinase phosphorylation of Drp1 regulates its GTPase activity and mitochondrial morphology. *J Biol Chem.* 2007;282:21583–21587.
47. Aldakkak M, Stowe DF, Heisner JS, et al. Enhanced Na⁺/H⁺ exchange during ischemia and reperfusion impairs mitochondrial bioenergetics and myocardial function. *J Cardiovasc Pharmacol.* 2008;52:236–244.
48. Rouslin W. Mitochondrial complexes I, II, III, IV, and V in myocardial ischemia and autolysis. *Am J Physiol.* 1983;244:H743–H748.
49. Chen Q, Hoppel CL, Lesnefsky EJ. Blockade of electron transport before cardiac ischemia with the reversible inhibitor amobarbital protects rat heart mitochondria. *J Pharmacol Exp Ther.* 2006;316:200–207.
50. Turner JD, Gaspers LD, Wang G, et al. Uncoupling protein-2 modulates myocardial excitation-contraction coupling. *Circ Res.* 2010;106:730–738.
51. Cabrera JA, Ziembra EA, Colbert R, et al. Altered expression of mitochondrial electron transport chain proteins and improved myocardial energetic state during late ischemic preconditioning. *Am J Physiol Heart Circ Physiol.* 2012;302:H1974–H1982.